

Dalton Transactions

Accepted Manuscript



This is an *Accepted Manuscript*, which has been through the Royal Society of Chemistry peer review process and has been accepted for publication.

Accepted Manuscripts are published online shortly after acceptance, before technical editing, formatting and proof reading. Using this free service, authors can make their results available to the community, in citable form, before we publish the edited article. We will replace this *Accepted Manuscript* with the edited and formatted *Advance Article* as soon as it is available.

You can find more information about *Accepted Manuscripts* in the [Information for Authors](#).

Please note that technical editing may introduce minor changes to the text and/or graphics, which may alter content. The journal's standard [Terms & Conditions](#) and the [Ethical guidelines](#) still apply. In no event shall the Royal Society of Chemistry be held responsible for any errors or omissions in this *Accepted Manuscript* or any consequences arising from the use of any information it contains.

Cite this: DOI: 10.1039/c0xx00000x

www.rsc.org/xxxxxx

ARTICLE TYPE

Photoreduction and light-induced triplet-state formation in a single-site fluoroalkylated zinc phthalocyanine

Hans Moons,^a Andrei Loas,^{b,c} Sergiu M. Gorun^{*b} and Sabine Van Doorslaer^{*a}

Received (in XXX, XXX) Xth XXXXXXXXX 2014, Accepted Xth XXXXXXXXX 2014

DOI: 10.1039/b000000x

Electron-withdrawing perfluoroalkyl peripheral substituents enhance the photosensitizing properties of metal phthalocyanines while increasing their solubility, thus providing opportunities for advanced characterization of their catalytically-relevant excited states. Optical absorption and electron paramagnetic resonance (EPR) spectroscopy experiments reveal that red light induces the reduction of perfluoroisopropyl-substituted zinc(II) phthalocyanine (F₆₄PcZn) dissolved in ethanol. A similar photoreduction does not occur in toluene. Furthermore, intense UV irradiation causes the photodegradation of F₆₄PcZn in ethanol, but low power UV illumination favours the formation of the triplet excited state, a prerequisite for new photocatalytic applications. The UV-induced triplet state of F₆₄PcZn is characterized using a combination of transient EPR experiments and DFT computations.

Introduction

Phthalocyanines (Pcs) are employed in a wide variety of applications.¹ Initially used as industrial dyes, they are currently investigated as state-of-the-art materials for implementation in molecular electronic devices, such as solar cells, or for use as photodynamic therapy agents. Moreover, the catalytic properties of these complexes are of interest.² The versatile phthalocyanine chemistry allows for fine tuning of their properties by variations of the Pc ring substituents and the central metal.¹ Previously, some of us have shown that by introducing perfluoroisopropyl (*i*-C₃F₇) peripheral substituents in the perfluorophthalocyanine ring to obtain 29*H*,31*H*,1,4,8,11, 15,18,22,25-octafluoro-2,3,9,10,16,17,23,24-octakis-perfluoro-isopropyl phthalocyanine (F₆₄PcH₂),³⁻⁴ one can easily produce molecules containing (i) closed shell ions zinc,^{2a} and magnesium,^{2b,c} (ii) open shell ions cobalt,⁵ and copper,⁶ as well as (iii) double-decker, lanthanide complexes,⁷ all of which yielded single crystals exhibiting long-range order. The enhanced solubility of these tridimensional perfluoroalkyl-perfluorophthalocyanines paved the way for many applications in catalysis^{2,8-10} and photodynamic therapy.⁴ Films and powders of different metal F₆₄Pcs exhibit only a small extent of intermolecular electronic coupling.^{6,11} This single-site isolation favors catalytic applications: F₆₄PcZn (Figure 1), for instance, is able to oxygenate external substrates,⁹ or, intercalated in bentonite as a hybrid photosensitizer, oxidatively degrade Acid Orange 7 in aqueous solutions under visible light.⁸

The triplet spin state of photoexcited F₆₄PcZn was shown to be sufficiently long living to render the complex a potential photosensitizer.⁵ In the absence of dioxygen, the lifetime of this state was found to be ~50 times longer than that of the perfluorinated analogue containing only F atoms, F₁₆PcZn, the key reason being most likely the lack of aggregation of the former complex, in contrast to the latter.

The formation of excited states is a key step toward reactivity and, therefore, their physical parameters are worth investigating. Amongst useful techniques, transient electron paramagnetic resonance (TREPR) is known to be a versatile tool to monitor the formation of photo-induced triplet states and radical pairs,^{12,13} and was used to identify and characterize the triplet state of photoexcited H₁₆PcZn, the parent, H-containing phthalocyanine, both in a frozen solution in 2-methyltetrahydrofuran and in powder form at low temperatures.¹⁴

We report the use of W-band TREPR in combination with density functional theory (DFT) computations to characterize paramagnetic species obtained from F₆₄PcZn following irradiation, viz. its triplet state generated via photoexcitation in frozen solutions and the [F₆₄PcZn]⁻ radical anion generated via photoreduction.

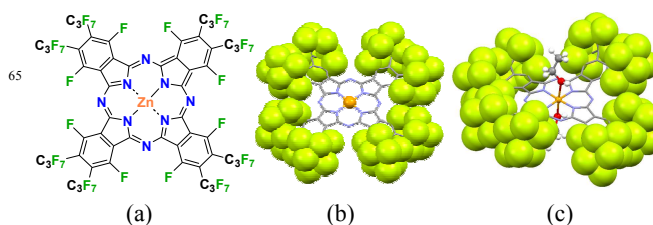


Fig. 1 (a) Structural formula of F₆₄PcZn; C₃F₇ = perfluoro isopropyl. (b) X-ray structure of F₆₄PcZn(acetone)₂.⁵ The axially coordinated acetone molecules have been omitted for the sake of clarity. (c) DFT-generated F₆₄PcZn(ethanol)₂. Color code: F, green, N, blue, C, gray, O, red, H, white. The F atoms are shown as van der Waals, spheres, the rest of the macrocycle atoms, with the exception of the Zn atom, are depicted as capped sticks. The Zn atom and the axial ligands are shown in ball-and-stick representation.

The anion radical was reported to have been obtained via the electrochemical reduction of F₆₄PcZn or via its photochemical reduction using sacrificial hydrazine hydrate.^{15,16} In the current

work, we show that the photochemical production of reactive radical species can be achieved in ethanol without the need of an external electron donor, an observation relevant to the previously reported photocatalytic properties of $F_{64}PcZn$ in ethanol.⁹

5 Experimental

Materials

Zinc(II) 1,4,8,11,15,18,22,25-octafluoro-2,3,9,10,16,17,23,24-octakis(perfluoroisopropyl-perfluorophthalocyanine) ($F_{64}PcZn$) was obtained and purified as described previously.⁵ For EPR measurements, absolute ethanol (Sigma-Aldrich) solutions of 1 mM $F_{64}PcZn$ were prepared. For optical absorption measurements, the solutions were diluted to a maximum absorbance below 2.

Optical absorption spectroscopy

UV-visible electronic absorption measurements were carried out on a Varian Cary 500 UV-Vis-NIR spectrophotometer using 1 cm quartz cells. If anaerobic conditions were required, the samples were prepared, transferred into the quartz cell and sealed in a glove box under a purified N_2 atmosphere. For the photoreduction experiments, the samples were irradiated with a 450 W Xe lamp (Edinburgh Instruments Xe900) prior to UV-visible absorption measurements. For the red light illumination, the Xe900 lamp was used with a 570 nm cut-off filter.

X-band continuous-wave EPR experiments

For the X-band CW EPR measurements, a Bruker ESP300E spectrometer (microwave frequency ~ 9.4 GHz) was used. The static magnetic field (0-1.5 T) was provided by a Varian V-7300 electromagnet. The field value was measured with a Bruker ER035M NMR gauss meter. The resonator was a Bruker ER 4102ST rectangular cavity operating in the TE_{102} mode. A modulation amplitude of 0.1 mT and a microwave power of 2 mW were used for the room-temperature experiments.

W-band transient EPR experiments

The W-band transient EPR experiments were performed at 50 K using a Bruker ELEXSYS E680 spectrometer equipped with a continuous helium flow cryostat and a superconductive split-coil magnet (0-6T, Oxford Instruments). The light source was a Nd:YAG laser (QuantaRay INDI, Spectra Physics, pulse width ~ 5 ns) operated in Q-switched mode at a 20 Hz repetition rate at 355 nm. The light was transported through a high-power silica fiber resulting in a power of approximately 0.25 mJ/pulse on the sample location. The EPR spectra were simulated using EasySpin, a Matlab toolbox.¹⁷

DFT computations

Spin-unrestricted DFT computations were performed using the ORCA package.¹⁸⁻²¹ Two $F_{64}PcZn$ species were modeled. Model A is the triplet state of $F_{64}PcZn$ in ethanol (no solvation) while Model B is the triplet state of the bis solvated species, $F_{64}PcZn(\text{ethanol})_2$. Figure 1b represents graphically Model A based on the $F_{64}PcZn(\text{acetone})_2$ structure with the axial ligands omitted. Figure 1c represents Model B based on the DFT coordinates. In order to simulate the solvent environment, a dielectric medium with the dielectric constant of ethanol

according to the COSMO model was used.²² For the geometry optimizations, the Becke-Perdew density functional (BP86)²³⁻²⁵ was used together with the resolution of the identity method.²⁶⁻²⁸ The split-valence plus polarization (SVP) basis set²⁹ was used for all atoms except for the zinc atom, in which case a more polarized triple zeta valence (TZVPP) basis was employed. The energy converged to 10^{-8} Hartree (Eh), with the convergence tolerances in the geometry optimization of 3×10^{-4} Eh/Bohr for the gradient and 5×10^{-6} Eh for the total energy. No symmetry constraints were used for the structure optimization. Single point calculations with the B3LYP functional³⁰ were carried out at the optimized geometries to predict the EPR spectral parameters. In these calculations, the "EPR-II" basis set³¹ was used for all atoms, except for the zinc ion, for which the (TZVPP) basis set was used. The zero-field splitting tensor was calculated taking the spin-spin interaction and the spin-orbit coupling into account.

70 Results and Discussions

Photo-stability and photo-reduction of $F_{64}PcZn$

The steady-state optical absorption spectra of $F_{64}PcZn$ in ethanol recorded in air (Figure S1) and under N_2 atmosphere (Figure 2) are similar to those previously reported for $F_{64}PcZn$ in DMF.^{15,16} When ethanolic solutions of $F_{64}PcZn$ were irradiated with UV light generated by a Xe lamp (450 W), a clear decrease in absorbance was observed under aerobic conditions, Figure S2; after 60 min of irradiation, the absorbance was reduced to about 80% of the original signal intensity. The limited stability of metal phthalocyanines under UV light has been reported earlier.^{32,33} Under these conditions, the stability of $F_{64}PcZn$ in ethanol can be considered good, given that some phthalocyanines are reported to almost fully degrade within an hour as a result of scattered daylight.³² For instance, 30 minutes of illumination of a $F_{16}PcZn$ solution in toluene in air resulted in only $\sim 30\%$ retention of the original signal intensity (not shown).

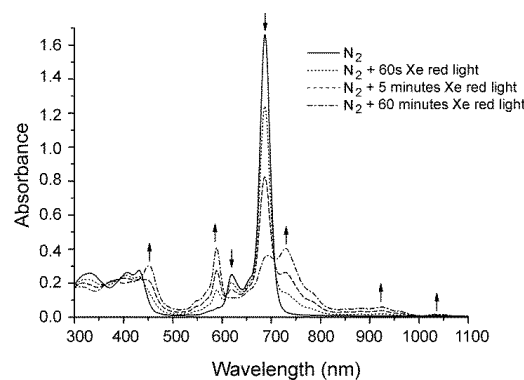


Fig. 2 Steady-state UV-visible spectra of $F_{64}PcZn$ in ethanol under N_2 atmosphere (solid line) and after successive irradiation with a 450 W Xe lamp equipped with a cut-off filter at 570 nm.

When the UV component of the Xe lamp radiation was filtered out with the aid of a 570 nm cut-off filter, illumination of an oxygen-free solution of $F_{64}PcZn$ in ethanol produced a surprising change in the absorption spectrum, identified as a photo-reduction to the ring-reduced radical anion species $[F_{64}PcZn]^-$ (Figure 2). The latter was assigned based on previously reported absorption bands characteristic of this species (upwards arrows,

Figure 2), which were also observed for the electrochemically reduced complex and the photo-reduced complex in the presence of sacrificial hydrazine hydrate^{15,16} (Table 1). The small hypsochromic shifts of the absorption maxima are due to the change of solvent. The photoreduction was found to be reversible: after oxygenation of the sample the initial optical spectrum of F₆₄PcZn in ethanol is regenerated (Figure S3). The experiment was repeated with full spectrum UV-visible light (450 W Xe lamp, Figure S5a). In contrast to the relatively slow build-up of [F₆₄PcZn]^{•-} observed under red-filtered light (Figures 2 and S4), complete photoreduction occurs within the first 3 minutes under UV-illumination (Figure S5). However, in this case, a slow F₆₄PcZn degradation also takes place. When F₆₄PcZn is dissolved in toluene, no reduction upon red light activation is observed (Figure S6).

The formation of the radical anion [F₆₄PcZn]^{•-} was further probed via EPR. Figure 3 shows the X-band CW-EPR spectrum of an anaerobic ethanol solution of red light-photoreduced F₆₄PcZn. A featureless signal around *g* = 2.003 is noted, typical of a radical and similar to the signal observed for [F₆₄PcZn]^{•-} generated photochemically in DMF in the presence of hydrazine hydrate.¹⁶ This result confirms that phthalocyanine ring reduction has occurred.

Electrochemical studies on metallophthalocyanines have shown that up to four electrons can be reversibly added to, or up to two electrons can be reversibly removed from the Pc macrocycle.³⁴ To the best of our knowledge, photoreduction of a zinc phthalocyanine using the solvent (ethanol) as the electron donor has never been reported before.

Table 1 Comparison between the absorption maxima of [F₆₄PcZn]^{•-} obtained via different reduction methods in ethanol and DMF

λ_{max} , nm	
Photoreduced F ₆₄ PcZn in ethanol (this work)	Photo-/electrochemically reduced F ₆₄ PcZn in DMF ¹⁶
452	468
589	594
729	743
924	not reported
1038	not reported

Earlier cyclic voltammetry studies have shown that F₆₄PcZn can be reduced electrochemically much easier than PcZn.¹⁶ The facile photoreduction of F₆₄PcZn in the presence of ethanol may be explained by an exacerbated Lewis acidity of the Zn ion induced by the electron-withdrawing perfluoroalkyl peripheral substituents, thus rendering the metal centre prone to axial coordination of ethanol ligands. This is in line with our earlier pulsed EPR studies on F₆₄PcCu that unambiguously proved binding of ethanol to this Cu(II) complex in solution.⁶ The coordination of ethanol may make an efficient inner-sphere electron transfer process possible, thus favouring the reduction of the complex.

The observation that a reduction does not take place for the complex in a non-coordinating solvent, like toluene (Figure S6), suggests that axial ligation indeed plays a crucial role in this process. The need for coordination of ethanol to the zinc phthalocyanine may also explain why the formation of

[F₆₄PcZn]^{•-} under red light illumination cannot be modeled by a mono-exponential fit (Figure S4). No reduction of the complex is observed in any solvent when oxygen is present. When air is contacted with either the red light- or UV-reduced samples, the restoration to the original optical spectrum takes place, but several hours are needed to reach completion (Figure S7). This observation suggests that the lack of detectable reduction under aerobic illumination is not due to fast re-oxidation of [F₆₄PcZn]^{•-} to F₆₄PcZn (with corresponding formation of O₂). Competitive reactions involving dioxygen seem to hamper [F₆₄PcZn]^{•-} formation, rather than quenching of the radical state. Most likely, the competing reaction is the efficient production of singlet oxygen, ¹O₂, *vide infra*.

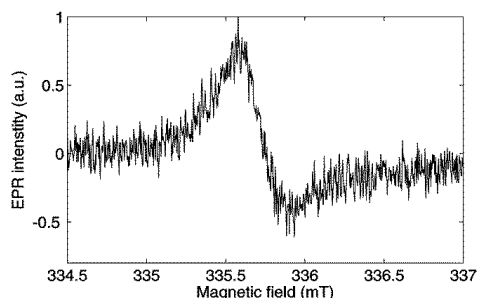


Fig. 3 Room temperature X-band CW EPR spectrum of the radical signal obtained under N₂ atmosphere immediately after illumination with red light of F₆₄PcZn in ethanol.

Triplet excited state formation

As mentioned above, F₆₄PcZn degrades in air under UV illumination, although its UV-stability is remarkably better than that reported for other zinc phthalocyanines. Earlier studies on PcZn and other metallophthalocyanines suggested that the following photochemical processes may be responsible for the photodegradation in air:³² (i) the phthalocyanine complex is excited from the S₀ to the S₁ state, which can be converted via inter-system crossing (ISC) in a triplet state (T₁), and (ii) the T₁ state reacts with ground-state oxygen, ³O₂, to produce ¹O₂ that may subsequently oxidize the macrocycle. A triplet excited state with a lifetime of 52 μs was determined following anaerobic red light illumination of 10 μM F₆₄PcZn in acetone.⁵ In the presence of oxygen, ¹O₂ is formed and higher tumor regression was observed during photodynamic therapy upon application of lower doses of photosensitizer when comparing F₆₄PcZn and PcZn *in vivo*.⁵ Furthermore, F₆₄PcZn is a much more efficient catalyst in the photooxidation of citronellol compared with other zinc phthalocyanines studied, owing to both its high quantum yield of ¹O₂ production and high photostability.⁹

In order to investigate whether the T₁ state is also induced in F₆₄PcZn under UV illumination, we performed transient EPR experiments. These measurements also allow for a determination of the spin Hamiltonian parameters of the T₁ state of F₆₄PcZn.

Cite this: DOI: 10.1039/c0xx00000x

www.rsc.org/xxxxxx

ARTICLE TYPE

Table 2 Experimental and DFT-computed g -values, zero-field splitting parameters for the T_1 state of $F_{64}PcZn$ in ethanol compared with other complexes, and structural comparison of experimental and modelled $F_{64}PcZn$ parameters.

Complex	g_x	g_y	g_z	$ D , \text{cm}^{-1}$	$ E , \text{cm}^{-1}$	Reference / Method	Macrocycle angles, $^\circ$	Zn-N bond lengths, \AA	Zn-O (axial) bond length, \AA
$F_{64}PcZn$ in ethanol	2.002 ^a	2.000 ^a	1.997 ^a	0.028 ^b	0.003 ^b	This work / TREPR	179.9 ^{c,e} 0.0 ^{d,e}	2.007 ± 0.003 ^c	2.422 ± 0.003 ^c
$F_{64}PcZn$ (Model A)	2.0032	2.0028	1.9978	0.0229	0.0011	This work / DFT	177.8 ± 0.2 ^{c,e} 4.7 ± 0.6 ^{d,e}	2.012 ± 0.008	-
$F_{64}PcZn(\text{EtOH})_2$ (Model B)	2.0032	2.0028	2.0004	0.0242	0.0037	This work / DFT	176 ± 1 ^{c,e} 21 ± 1 ^{d,e}	2.04 ± 0.01	2.310
$PcZn$ in 2-methyl-THF	2.008	2.004	2.002	0.025	0.004	14 / TREPR	-	-	-
tbPcZn ^f in Tol:CHCl ₃	n.r.	n.r.	n.r.	0.024	0.005	35 / TREPR	-	-	-
tbPcZn ^f in Tol:CHCl ₃	n.r.	n.r.	n.r.	0.025	0.002	35 / TREPR	-	-	-
ZnTPP ^g in Tol:CHCl ₃	n.r.	n.r.	n.r.	0.031	0.009	36 / TREPR	-	-	-

^aExperimental error = 0.001; ^bExperimental error = 0.002 cm^{-1} ; ^cThe average of the 2 Ct-Zn-Ct angles, where Ct are the geometric centers of the *trans* benzene rings; ^dThe average of the dihedral angles made by *trans* benzene rings; ^eThese experimental values refer to the isoelectronic $F_{64}PcZn(\text{acetone})_2$; ^ftbPc = tetra-tertbutyl phthalocyanine; ^gTPP = tetra phenyl porphyrin; Tol = toluene; n.r. = not reported.

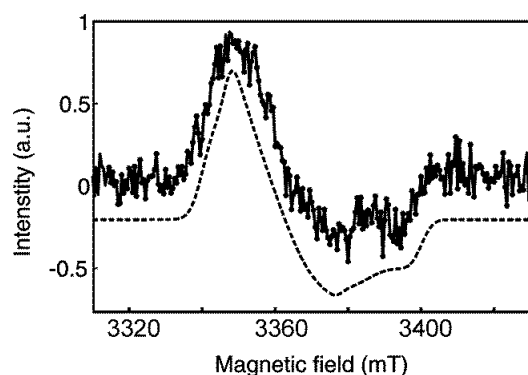


Fig. 4 W-band transient EPR spectrum of $F_{64}PcZn$ in ethanol at 50 K (solid line) and its simulation (dashed line), taken $\sim 1.5 \mu\text{s}$ after photo-excitation with a laser flash at 355 nm.

Although photodecomposition was observed under strong UV irradiation, low-temperature TREPR experiments could be performed with negligible degradation when exciting the molecule at 355 nm with a relatively low power laser light. Indeed, at low temperature, the diffusion rate of oxygen into the solution, which could be responsible for the quenching of the radical, is reduced and the magnetization dephasing occurs on a much faster time scale than oxygen diffusion.¹⁴

Figure 4 shows the photo-excited triplet state of $F_{64}PcZn$ in ethanol detected at 50 K with W-band TREPR. The spectrum may also be simulated, including the electron Zeeman term and the zero-field splitting assuming the spin Hamiltonian:

$$\hat{H} = \beta_e B_0 g \hat{S}_z + D \left(\hat{S}_z^2 - \frac{1}{3} \hat{S}^2 \right) + E \left(\hat{S}_x^2 - \hat{S}_y^2 \right) \quad (1)$$

The g -tensor has principal values g_x , g_y and g_z , B_0 is the external magnetic field, β_e is the Bohr magneton and D and E are the zero-field parameters. The best fit parameters are reported in Table 2, while the simulation is shown in Figure 4. The population distribution of the levels is set to 0:0:1 for $p_x:p_y:p_z$ in the simulation. D is assumed to be positive in accordance with the parent ZnPc¹⁴ and E is also taken positive in the simulation. The values are in the same order of magnitude as those earlier observed for solutions of the parent ZnPc and other zinc phthalocyanines and porphyrins^{14,35,36} (Table 2). In the frozen solution, the T_1 state of $F_{64}PcZn$ is formed via the conventional ISC process from the S_1 state. The population distribution indicates a preferential occupation of the lowest out-of-plane sublevel, provided that the zero-field splitting axes and the g tensor axes coincide. A dominant ISC to the out-of-plane sublevels was also reported.³⁵

The D values of metal Pcs are generally lower than those of the corresponding porphyrin complexes due to an extended delocalization of the unpaired π electrons in the T_1 state.³⁵ The D value of the triplet state of $F_{64}PcZn$ is, however, higher than those found for other metal Pcs (Table 2). It has been shown earlier that axial ligation may influence the zero-field splitting parameters of metal porphyrins.³⁵ Ethanol ligation may thus be responsible for the increased D value observed for the T_1 state of $F_{64}PcZn$, although the effect of the electron-withdrawing perfluoroalkyl substituents could also play a role.

In order to elucidate this further, DFT computations of the spin Hamiltonian parameters of the triplet state of $F_{64}PcZn$ in ethanol (Model A) and on $F_{64}PcZn(\text{ethanol})_2$ in ethanol (Model B) were performed. The computed g values and zero-field splitting parameters are shown in Table 2, along with the experimental ones.

The spin density distribution (Figure 5) of the triplet state of Model B explains the small, but non-negligible E value. The 4-

fold axis is lost but two orthogonal mirror planes containing the O(ethanol)-Zn-O(ethanol) axis are noted.

Surprisingly, although smaller than the equivalent value for Model B, the computed E value of Model A was also not zero.

Since no symmetry constraints were imposed during the geometry optimization, small differences in the *iso*-C₃F₇ substituents rotational positions, which break the symmetry, may contribute to the non-zero E value. It should be noted that DFT computations on the singlet and triplet states of PcZn also showed a decrease in symmetry from D_{4h} (ground state S₀) to D_{2h} in the triplet state.³⁷ In fact, all reported experimental E values for zinc phthalocyanines (Table 2) are non-zero.

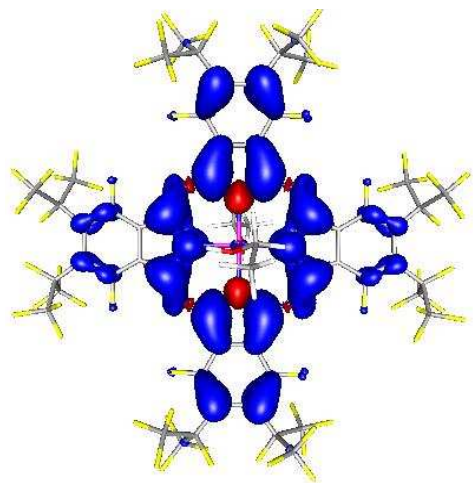


Fig. 5 Spin density distribution of the triplet state of F₆₄PcZn(ethanol)₂ in ethanol, Model B, viewed along the O(ethanol)-Zn-O(ethanol) axis. Blue: positive spin density; red: negative spin density.

Perhaps more importantly than the break of the D_{4h} symmetry due to the restricted rotations of the *iso*-C₃F₇ groups, Pc rings distortions may be anticipated due to axial coordination. The geometrical features of Models A and B reveal the anticipated distortions. Thus, a comparison between the calculated geometries, based on the coordinates of the optimized geometries (see the ESI) and the experimental observations for F₆₄PcZn(acetone)₂, Figure S9 and Table S1 reveal that the DFT-generated geometry the F₆₄PcZn(ethanol)₂ complex exhibits a saddle distortion (Figure 1c). One can estimate the macrocycle distortions by computing their Ct-Zn-Ct angles, where Cts are the geometric centers of *trans* benzene rings. For lack of distortions, the angle should be 180°, as is indeed observed for F₆₄PcZn(acetone)₂, Table 2. In contrast, this angle is 177.8 ± 0.2 and 176 ± 1° for Models A and B, respectively, proving the existence of saddle distortions. A second type of distortion, which also affects the degree of the π conjugation, is represented by the dihedral angles made by the *trans* benzene rings. While this distortion is absent in F₆₄PcZn(acetone)₂, it is about 5° in Model A, which lacks axial ligands. In contrast, Model B, which displays bis-axial ethanol coordination, Figure 1c, exhibits a severe distortion, 21°, thus breaking the 4-fold axial symmetry. Notably, ethanol coordination also distorts the ZnN₄ chromophore of Model B relative to that of both Model A and the similarly coordinated, as illustrated by the goodness-of-fit of the overlaid structures, Figure S9 and Table S1. The effects of bis axial coordination are difficult to assess accurately, since there

are no *trans* bis acetone or ethanol complexes reported in the Cambridge Crystallographic Database (2014), with the exception of F₆₄PcZn(acetone)₂.⁵ A review of axially ligated acetone and ethanol complexes exhibiting either equatorial N₄ or N₂O₂ coordination, Tables S2 and S3, reveals in both cases a lengthening of the Zn-O bond by ~0.06 Å on going from acetone to ethanol, reaching an average of 2.20 Å. The corresponding, larger value of 2.445 Å encountered in F₆₄PcZn(acetone)₂ is likely due to the addition of the sixth, *trans* ligand. This addition and the resulting *trans* effect suggest that the ethanol ligand is labile. The symmetry features, taken together, establish the origins of the spin density distribution mostly in the Pc ring distortions, given that the tertiary F groups are out of the Pc plans in Models A and B removing the mirror symmetry elements.

The computed zero-field splitting parameters in Table 2 agree well with the observed experimental values, and the DFT computations suggest that axial ligation indeed leads to a larger D value. However, one has to be careful in relying too strongly on a quantitative comparison between DFT and experimental results, since the agreement may be coincidental; DFT computation of zero-field splitting parameters for transition metals remains problematic.³⁸⁻⁴⁰ Present-day DFT methods rely on spin-unrestricted single-determinant methods, which are reasonably accurate for one-electron spin-dependent properties. However, they do not accurately reproduce the two-electron spin-dependent properties like the zero-field splitting.⁴¹ Yet, the geometrical predictions of the DFT calculations are consistent with the experimental observations. For an accurate calculation of zero-field splitting parameters, it is necessary to use correlated *ab initio* methods, which is beyond the scope of this contribution. Note that, even though the symmetry of the g tensor is correctly predicted, its principal values deviate significantly from the experimental ones, illustrating further the inherent difficulties in performing reliable DFT computations.

In this respect, it is interesting to note that the experimental g_z value of the T₁ state of F₆₄PcZn in ethanol is considerably lower than the free-electron g value (2.0023). This was not observed for PcZn in 2-methyl-THF.¹⁴ In fact, also the average isotropic g value is larger in the latter case. Although it is unclear at present what causes this difference, we should remark that the measurements in ref. 14 were performed at X-band, resulting in a reduced g resolution and a larger experimental error on the principal g values than when W-band microwave frequencies are used. Furthermore, although one should be careful when performing quantitative comparisons between experiment and DFT (*vide supra*), a g_z value below 2.0023 was predicted for both model A and B (Table 2), suggesting that this is an intrinsic property of the system under study.

Consequences for applications

Our observation that F₆₄PcZn can be anaerobically reduced by red light in the presence of only ethanol is unprecedented for phthalocyanines. Photoreduction has been observed for other phthalocyanines but always in the presence of strong electron donors, such as azaferrocene, hydrazine and different amines.^{16,42-44} The possibility of anaerobically reducing a Pc ring in the presence of an alcohol (in other words, oxidizing the solvent) opens new reactivity pathways. Simple oxygenation restores the neutral F₆₄PcZn molecule.

The related $F_{64}PcCo$ complex has already been shown to exhibit unusual chemistry, being able to catalytically reduce oxygen¹⁰ and couple phosphanes with acetone to form ylides.^{2a} Key to this unusual behavior seems to be the electron-withdrawing effect of the *iso*- C_3F_7 peripheral substituents. These substituents not only render the complexes readily soluble in organic solvents, but also favor axial binding to the central metal of ligands with lower coordinating power, such as alcohols.

Although $F_{64}PcZn$ dissolved in ethanol was found to degrade in air under strong UV irradiation, its stability is much improved with respect to other phthalocyanines and does not affect its favorable catalytic properties.⁹ Earlier studies indicated that both the molecular structure and the solvent play a crucial role in UV stability.³² The bridging aza nitrogen atoms form the weakest point in the Pc ring. Effective σ -donors were found to raise the electron density of the conjugated C–N bonding system and enhance the chemical stability.³² Ethanol ligation may thus actively promote the UV stability of the $F_{64}PcZn$ complex.

Finally, zinc phthalocyanines and porphyrins have been long contemplated as photosensitizers for medical applications.⁴⁵ A good candidate in this field has to fulfill several key requirements, including high stability, high solubility, low photodegradation, low toxicity and an efficient formation of the T_1 state leading to evolution of 1O_2 . The excited triplet state of $F_{64}PcZn$ forms readily and bears similar zero-field splitting parameters to other Pc and porphyrin derivatives, but has the added advantage of improved solubility in polar solvents.

Conclusions

In an oxygen-free environment, $F_{64}PcZn$ is readily reduced in ethanol under red light illumination, a rare phenomenon not encountered for other metallophthalocyanine analogues or in non-coordinating solvents, such as toluene. The photoreduction of the phthalocyanine ring is facilitated by axial ligation of ethanol, a process mediated by the strong electron-withdrawing effects of the perfluoroalkyl peripheral substituents, which enhance the Lewis acidity of the central metal.

Although intense UV illumination leads to a photodegradation of the complex in ethanol, photostability is greatly enhanced compared to related PcZn derivatives. The photo-excited T_1 state of $F_{64}PcZn$ in ethanol has zero-field parameters that are indicative of axial ethanol ligation, consistent DFT calculations of spin density distributions on solvated and unsolvated model complexes, as well as with a bis-ligated solid-state X-ray structure. The possibility of anaerobically and reversibly reducing the Pc ring while subsequently oxidizing substrates may open new avenues in catalytic chemistry.

Acknowledgment

Partial support from the National Science Foundation (SMG) is gratefully acknowledged.

Notes and references

^a University of Antwerp, Department of Physics, Universiteitsplein 1, 2610 Antwerp, Belgium. E-mail: sabine.vandoorslaer@ua.ac.be

^b Center for Functional Materials and Department of Chemistry and Biochemistry, Seton Hall University, South Orange, NJ 07079, USA

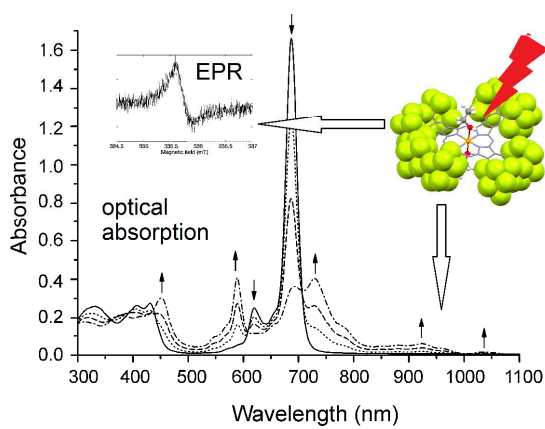
⁵⁵ E-mail: sergiu.gorun@shu.edu

^c Department of Chemistry, Massachusetts Institute of Technology, Cambridge, MA 02139, USA

† Electronic Supplementary Information (ESI) available: electronic spectra of $F_{64}PcZn$, UV degradation experiments, kinetic and structural modeling data, structural parameters of ZnN_2O_2 and ZnN_4 chromophores, DFT results. See DOI: 10.1039/b000000x/

1. N. B. McKeown, *Phthalocyanine Materials: Synthesis, Structure and Function*, Cambridge University Press, Cambridge, 1998.
2. (a) B. A. Bench, W. W. Brennessel, H.-J. Lee and S. M. Gorun, *Angew. Chem.Int. Ed.*, 2002, **41**, 750; (b) S. V. Dugan, Ł. Łapok, P. Zimcik, V. Novakova, A. Tochtenhagen, M. Hintsche, C. Litwinski, B. Roder, H. Patel and S. M. Gorun, Pub. #228, 245th ACS National Meeting, New Orleans, April 7-11, 2013. (c) S. V. Dugan, Ł. Łapok, A. Tochtenhagen, M. Hintsche, C. Litwinski, B. Roder, H. Patel, K. A. Griswold, J. Zunino and S. M. Gorun, to be submitted.
3. H.-J. Lee, W. W. Brennessel, J. A. Lessing, W. W. Brucker, V. G. Young and S. M. Gorun, *Chem. Commun.*, 2003, 1576.
4. R. Minnes, H. Weitman, H.-J. Lee and S. M. Gorun, *Photochem. Photobiol.*, 2006, **82**, 593.
5. B. A. Bench, A. Beveridge, W. M. Sharman, G. J. Diebold, J. E. Van Lier and S. M. Gorun, *Angew. Chem.Int. Ed.*, 2002, **41**, 748.
6. H. Moons, Ł. Łapok, A. Loas, S. Van Doorslaer, S. M. Gorun, *Inorg. Chem.*, 2010, **49**, 8779.
7. M. Gonidec, I. Krivokapic, J. Vidal-Gancedo, E. S. Davies, J. McMaster, S. M. Gorun and J. Veciana, *Inorg. Chem.*, 2013, **52**, 4464.
8. D. Drozd, K. Szczubiałka, Ł. Łapok, M. Skiba, H. Patel, S. M. Gorun and M. Nowakowska, *Appl. Catal. B*, 2012, **125**, 35.
9. R. Gerdes, Ł. Łapok, O. Tsaryova, D. Wöhrle and S. M. Gorun, *Dalton Trans.*, 2009, 1098.
10. A. Loas, R. Gerdes, Y. Zhang and S. M. Gorun, *Dalton Trans.*, 2011, **40**, 5162.
11. C. Keil, O. Tsaryova, C. Himeinshi, D. Wöhrle, O. R. Hild, D. R. T. Zahn, S. M. Gorun and D. Schlettwein, *Thin Solid Films*, 2009, **517**, 4379.
12. P. Atkins, K. McLaughlan and P. Percival, *Mol. Phys.*, 1973, **25**, 281.
13. A. van der Est, *Photosynth. Res.*, 2009, **102**, 335.
14. A. Barbon, M. Brustolon, E. E. van Faassen, *Phys. Chem. Chem. Phys.*, 2001, **3**, 5342.
15. S. P. Keizer, W. Han, M. J. Stillman, *Inorg. Chem.*, 2002, **41**, 353.
16. S. P. Keizer, J. Mack, B. A. Bench, S. M. Gorun and M. J. Stillman, *J. Am. Chem. Soc.*, 2003, **125**, 7067.
17. S. Stoll and A. Schweiger, *J. Magn. Reson.*, 2006, **178**, 42.
18. F. Neese, *J. Chem. Phys.*, 2001, **115**, 11080.
19. F. Neese, *J. Phys. Chem. A*, 2001, **105**, 4290.
20. F. Neese, *J. Chem. Phys.*, 2003, **118**, 3939.
21. F. Neese, *J. Chem. Phys.*, 2005, **122**, 034107/1.
22. S. Sinnecker, A. Rajendran, A. Klamt, M. Diedenhofen and F. Neese, *J. Phys. Chem. A*, 2006, **110**, 2235.
23. A. D. Becke, *Phys. Rev. A*, 1988, **38**, 3098.
24. J. P. Perdew, *Phys. Rev. B*, 1986, **33**, 8822.
25. J. P. Perdew, *Phys. Rev. B*, 1986, **34**, 7406.
26. B. I. Dunlap, J. W. D. Connolly and J. R. Sabin, *J. Chem. Phys.*, 1979, **71**, 3396.
27. K. Eichkorn, O. Treutler, H. Ohm, M. Haser and R. Ahlrichs, *Chem. Phys. Lett.*, 1995, **240**, 283.
28. O. Vahtras, J. Almlöf and M. W. Feyereisen, *Chem. Phys. Lett.*, 1993, **213**, 514.
29. A. Schäfer, H. Horn and R. Ahlrichs, *J. Chem. Phys.*, 1992, **97**, 2571.
30. P. J. Stephens, F. J. Devlin, C. F. Chabalowski and M. J. Frisch, *J. Phys. Chem.*, 1994, **98**, 11623.
31. V. Barone, *Recent Advances in Density Functional Methods*, World Scientific Publ. Co., Singapore, 1996.
32. R. Slota and G. Dyrda, *Inorg. Chem.*, 2003, **42**, 5743.

33. T. Caronna, C. Colleoni, S. Dotti, F. Fontana and G. Rosace, *J. Photochem. Photobiol. A*, 2006, **184**, 135.
34. J. Mack and M. J. Stillman, *Inorg. Chem.*, 1997, **36**, 413.
- 5 35. K. Ishii, S. Abiko and N. Kobayashi, *Inorg. Chem.*, 2000, **39**, 468.
36. K. Akiyama, S. Terokubota and Y. Ikegami, *Chem. Phys. Lett.*, 1991, **185**, 65.
37. L. T. Ueno, C. C. Jayme, L. R. Silva, E. B. Pereira, S. M. de Oliveira and A. E. H. Machado, *J. Braz. Chem. Soc.*, 2012, **23**, 2237.
- 10 38. F. Neese, *Coord. Chem. Rev.*, 2009, **253**, 526.
39. *Calculation of NMR and EPR Parameters. Theory and Applications*, eds. M. Kaupp, M. Bühl and V. G. Malkin, Wiley-VCH Verlag, Weinheim, 2004.
- 15 40. F. Neese, *J. Biol. Inorg. Chem.*, 2006, **11**, 702.
41. M. van Gastel, *J. Chem. Phys.*, 2009, **131**, 7.
42. Y. Kaneko, T. Arai, H. Sakuragi, K. Tokumaru and C. Pac, *J. Photochem. Photobiol. A*, 1996, **97**, 155.
- 20 43. Y. Kaneko, Y. Nishimura, T. Arai, H. Sakuragi, K. Tokumaru and D. Matsunaga, *Photochem. Photobiol. A*, 1995, **89**, 37.
44. J. Zakrzewski and C. Giannotti, *Inorg. Chim. Acta*, 1995, **232**, 63.
- 25 45. *Photosensitizers in Medicine, Environment and Security*, eds. T. Nyokong and V. Ahsen, Springer Science, London, 2012.



Anaerobic red-light illumination leads to reduction of perfluoroisopropyl-substituted zinc(II) phthalocyanine in ethanol, while low power UV illumination favours the formation of a triplet excited state.